EUROPEAN ORGANIZATION FOR NUCLEAR RESEARCH

CERN-OPEN-2001-028
February 24, 1998

Beam Measurements of a CLOUD (Cosmics Leaving OUtdoor Droplets) Chamber

Jasper Kirkby
CERN, Geneva, Switzerland

Abstract

A striking correlation has recently been observed between global cloud cover and the flux of incident cosmic rays. The effect of natural variations in the cosmic ray flux is large, causing estimated changes in the Earth's energy radiation balance that are comparable to those attributed to greenhouse gases from the burning of fossil fuels since the Industrial Revolution. However a direct link between cosmic rays and cloud formation has not been unambiguously established. We therefore propose to experimentally measure cloud (water droplet) formation under controlled conditions in a test beam at CERN with a CLOUD chamber, duplicating the conditions prevailing in the troposphere. These data, which have never been previously obtained, will allow a detailed understanding of the possible effects of cosmic rays on clouds and confirm, or otherwise, a direct link between cosmic rays, global cloud cover and the Earth's climate. The measurements will, in turn, allow more reliable calculations to be made of the residual effect on global temperatures of the burning of fossil fuels, an issue of profound importance to society. Furthermore, light radioisotope records indicate a correlation has existed between global climate and the cosmic ray flux extending back over the present inter-glacial and perhaps earlier. This suggests it may eventually become possible to make long-term (10–1,000 year) predictions of changes in the Earth's climate, provided a deeper understanding can be achieved of the "geomagnetic climate" of the Sun and Earth that modulates the cosmic-ray flux.

Contents

1 Introduction

Global warming is a major concern of the world, with its potentially devastating effects on coastal settlements and world agriculture. The steep rise in greenhouse gas emissions since the Industrial Revolution has increased the CO_2 concentration in the atmosphere by 30% (Fig. 1). This is widely believed to be the dominant cause of the observed rise of about 0.6°C in the global mean surface temperature during this period (Fig. 2) [1].

A small systematic rise or fall in the global temperature is caused by a net imbalance ("forcing") in the Earth's energy radiation budget (Fig. 3). The radiative forcing caused by the increase in the CO_2 fraction since 1750 is estimated to be 1.5 Wm^{-2} [1], compared with the global average incoming solar radiation of 342 Wm^{-2}, i.e. an imbalance of only 0.4%. After including the effects of all greenhouse gases (+2.45 Wm^{-2}), aerosols[1] (-0.5 Wm^{-2}) and their effects on clouds (-0.75 Wm^{-2}), the present net radiative forcing from mankind is estimated to be 1.2 Wm^{-2}.

The climate models [1] upon which the predictions of greenhouse warming depend have gradually improved as new effects and better data have been incorporated. They now provide a reasonable representation of the observed variation in global temperature over the last century (Fig. 2). However they remain subject to significant uncertainties, both from unknown processes and also from the unknown effects of feedback mechanisms which may amplify or damp a warming trend. Important unknown effects include those due to increased evaporation of water (which may cool due to an increased cloudiness or warm due to an increased greenhouse effect), shifts in the amount of CO_2 dissolved in the oceans, changes in the ocean currents and changes in the polar ice. Given the uncertainties in these models, many scientists consider there is no convincing evidence at present to demonstrate that a greenhouse warming of the planet is in progress, let alone that the models can reliably predict future temperature changes (the predicted rise by the end of the next century is 1.3–2.5°C; Fig. 4).

Nonetheless it is in this climate of scientific uncertainty that major political decisions on greenhouse gas emissions are presently being made (Earth Summit in Rio de Janeiro, 1992, and UN Climate Convention in Kyoto, 1997) that will have a profound effect on the economic development of both the developed and the developing countries. The need for such political decisions to be based on sound scientific grounds is self evident, and a major world-wide research effort on climate change is underway.

An unexpected and important factor in climate change has recently been discovered: cloud cover seems to follow natural variations in the incident cosmic ray flux [2, 3]. However a direct link between cosmic rays and cloud formation has not been unambiguously established and, moreover, the microphysical mechanism is poorly understood. This presents particle physics with a unique opportunity to make a major contribution to the problem of global warming by confirming, or otherwise, this link under controlled conditions in a test beam. The purpose of this paper is to provide an initial outline of the motivation and conceptual design of the proposed CLOUD (Cosmics Leaving OUtdoor Droplets) detector.

[1]Aerosols are 0.001–1 μm diameter particles of liquid or solid in suspension. Atmospheric aerosols include dust, sea salt, soot (elemental carbon), organic compounds from biomass burning, sulphates (especially $(NH_4)_2SO_4$) from SO_2, and nitrates from NO and NO_2. Aerosol concentrations vary from a few per cm^3 in clean maritime air to 10^6 cm^{-3} in highly-polluted city air.

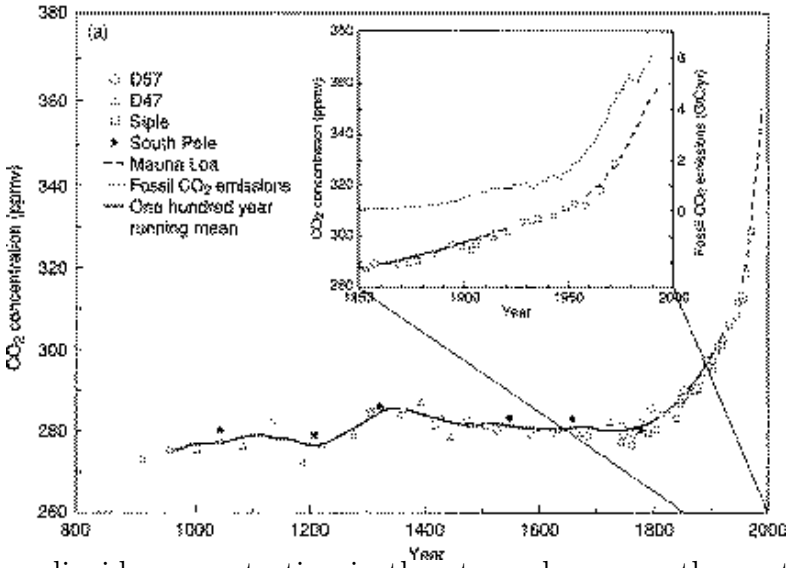

Figure 1: Carbon dioxide concentration in the atmosphere over the past 1000 years [1]. The data are based on Antarctica ice core records and, since 1958, on direct measurements from Mauna Loa, Hawaii. Also shown are the estimated yearly emissions of CO_2 from burning fossil fuels since the Industrial Revolution.

2 The origins of climate change

The Earth's climate has not always been the same; significant changes have occurred during recorded history and even greater changes have taken place since the human ancestral line began about 5 million years ago. The urgent questions facing science are why these natural changes took place and whether there is currently an influence of mankind on the climate. Only when the natural causes are understood and properly accounted for in climate models can we expect meaningful results on the anthropogenic influences.

Several natural effects are well established. These include the Milankovitch cycles—variations in the Earth's orbit, tilt and spin with respect to the Sun—which seem to control the timing of glacials and interglacials. These cold and warm phases correspond to cycles of about 100,000 years and 10,000 years, respectively. (We are presently approaching the end of an interglacial; sometime in the next 1000 years or so the climate will probably become much colder.) Other important natural sources of climate change are the anomalous warm Pacific current known as El Niño, and volcanoes that pour ash into the stratosphere, reducing the radiation from the Sun reaching the Earth's surface. A recent volcanic example is Mt. Pinatubo in the Philippines, which erupted in June 1991 and caused a global cooling, by up to 0.4°C, over a period of about 3 years. In contrast, a natural effect that has until recently been harder to understand is the apparent link between solar activity—the sunspot[2] cycle—and the weather.

[2]Sunspots are areas of the Sun's photosphere where strong local magnetic fields (typically 2500 gauss, to be compared with the Earth's field of about 0.3 gauss) emerge vertically [4]. They appear dark because their temperature is about half of the surrounding photosphere (3,000 K compared with 5,800 K). They are thought to be generated by the different rotation rates of regions of the Sun: one revolution takes 25 days at the equator and 28 days at mid-latitudes. This modifies the normal convective motions of the plasma and creates "knots" of strong magnetic field which penetrate the photosphere and provide escape paths for the plasma, forming sunspots.

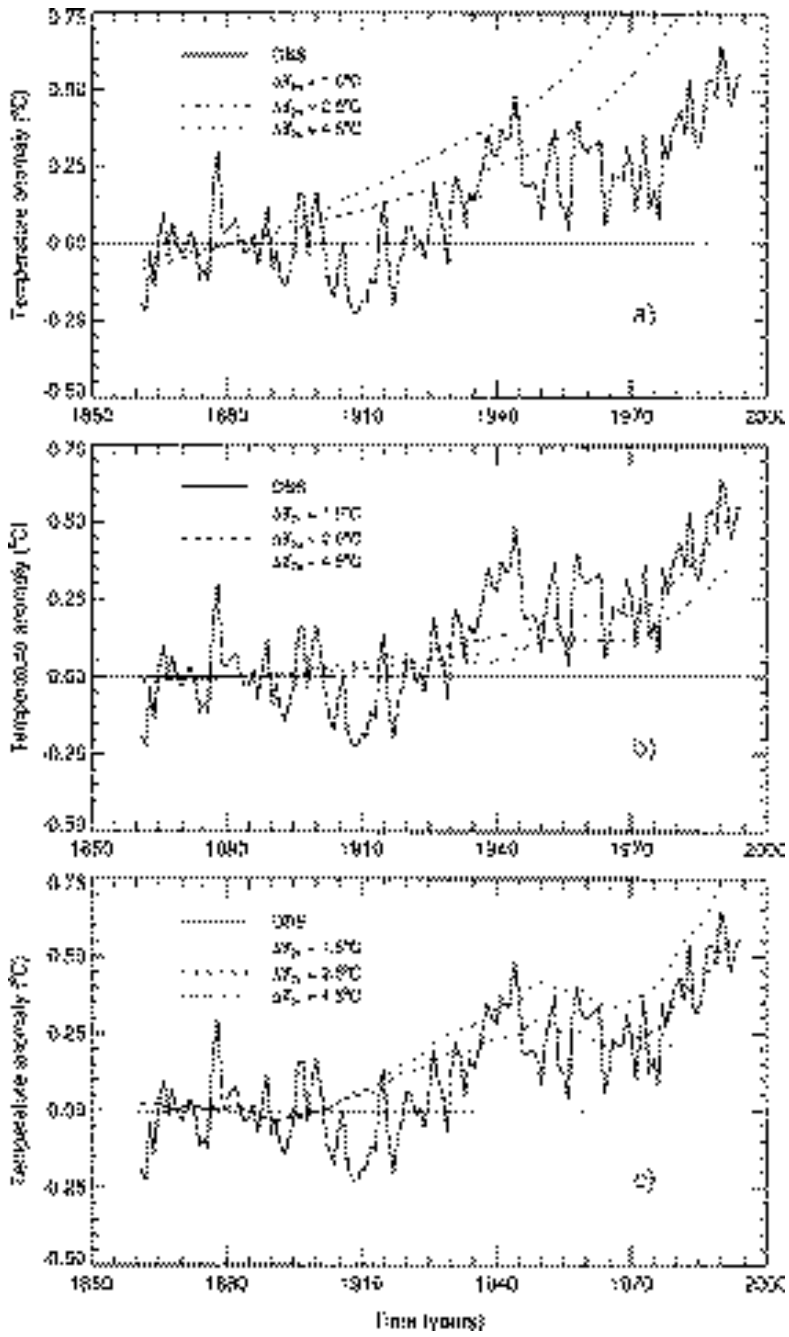

Figure 2: Observed changes in global mean surface temperature from 1861 to 1994, compared with the climate model of the Intergovernmental Panel on Climate Control (IPCC) on the effects of greenhouse gas emissions [1]. The model was run with a) greenhouse gases alone, b) greenhouse gases and aerosols, and c) greenhouse gases, aerosols and an estimate of changes in solar irradiance. The broken curves are the model predictions under several different assumptions of the climate sensitivity, $\Delta T_{2\times}$, which is the change in global mean temperature for a doubling of the atmospheric CO_2.

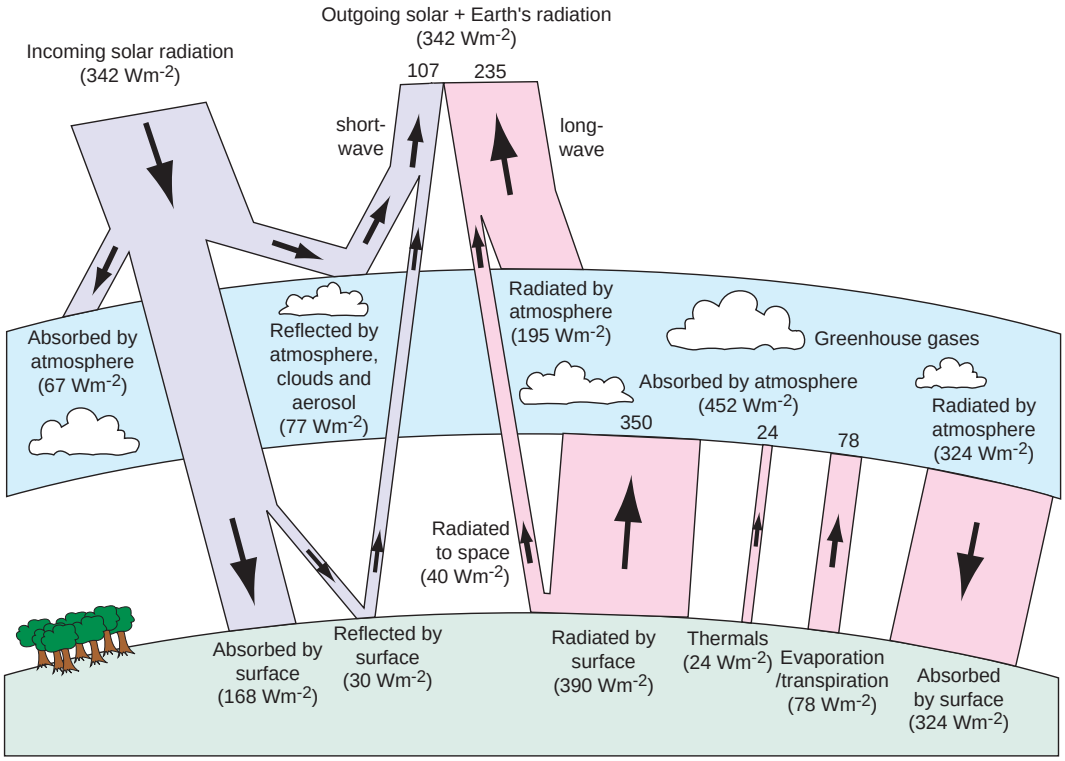

Figure 3: The Earth's energy radiation budget. The width of each band is proportional to the associated energy flux, which is computed as a global annual mean. Heat absorbed by the atmosphere produces a greenhouse effect since the radiation lost to space comes from the cold tops of clouds and from parts of the atmosphere much colder than the surface. The figure is adapted from reference [1].

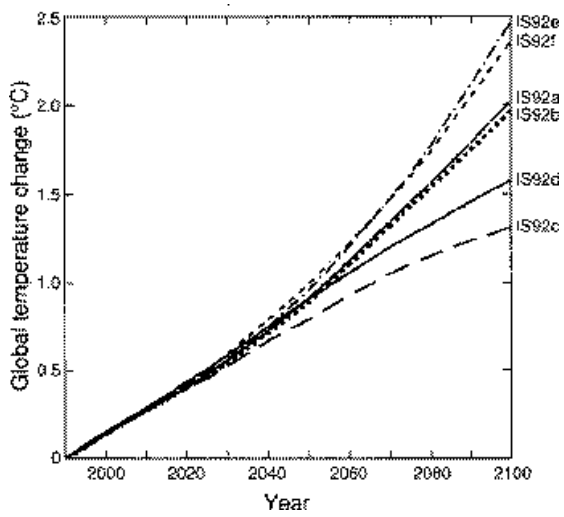

Figure 4: Projected global mean surface temperatures from 1990 to 2100 based on the current IPCC climate model (Fig. 2c) for the full set of IS92 CO_2 emission scenarios [1]. A climate sensitivity, $\Delta T_{2\times} = 2.5°\text{C}$, is assumed.

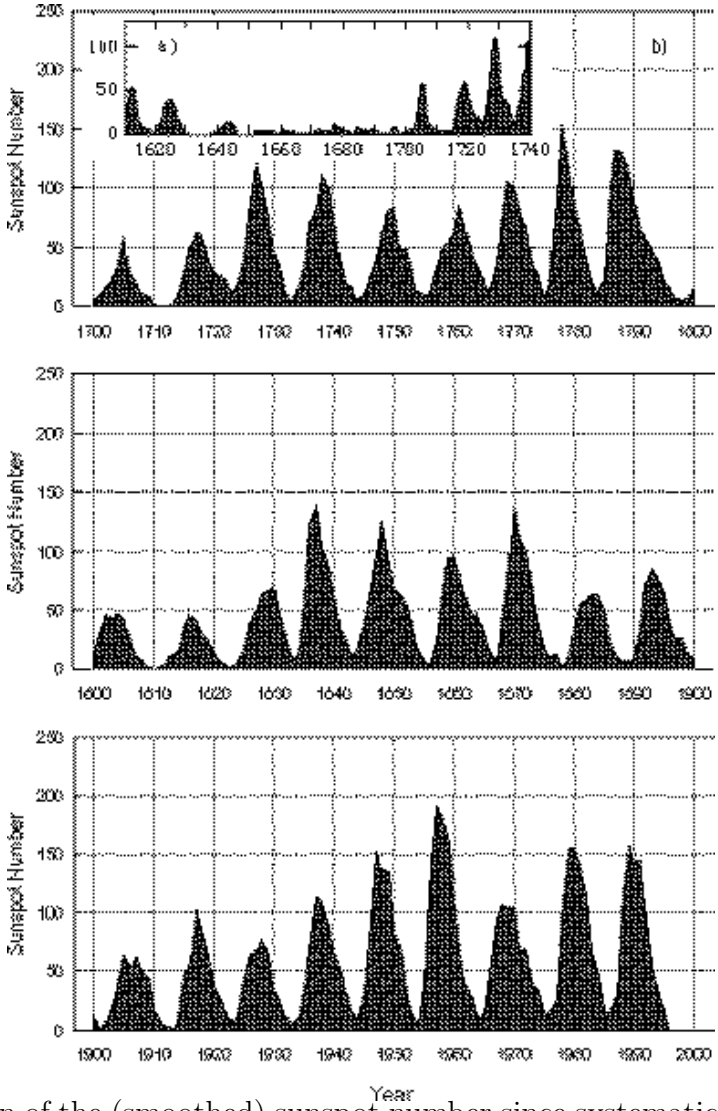

Figure 5: Variation of the (smoothed) sunspot number since systematic (telescope) observations began. The data show a) the period 1610–1740 [5] and b) the period 1700–1995 [the data are from NOAA—the National Oceanic and Atmospheric Administration].

2.1 Activity of the Sun

The observation that warm weather seems to coincide with high sunspot counts and cool weather with low sunspot counts was made as long ago as two hundred years by the astronomer William Herschel who noticed that the price of wheat in England was lower when there were many sunspots, and higher when there were few. The most well-known example of this effect is known as the Maunder Minimum [5], the Little Ice Age between 1645 and 1715—which ironically almost exactly coincides with the reign of Louis XIV, *le Roi Soleil*, 1643–1715—during which time there was an almost complete absence of sunspots (Fig. 5a). During this period the River Thames in London regularly froze across and fairs complete with swings, sideshows and food stalls were a standard winter feature.

Quantitative proof of a correlation between the Sun's activity and the Earth's temperature was presented by Friis-Christensen and Lassen [6] in 1991. They used the sunspot

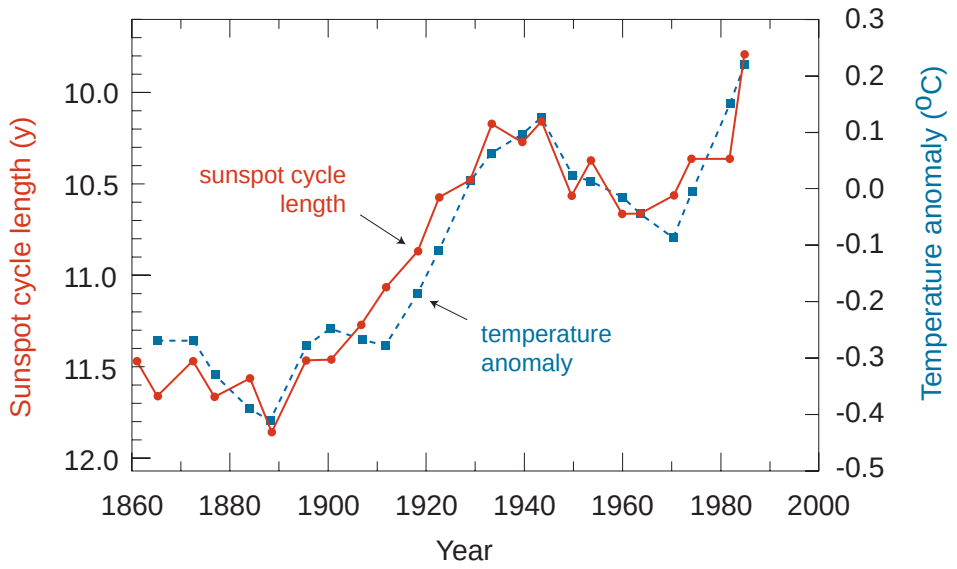

Figure 6: Variation during the period 1861–1989 of the sunspot cycle length (solid curve) and the temperature anomaly of the Northern Hemisphere (dashed curve) [6]. The temperature data from the IPCC [1].

cycle length as a measure of the Sun's activity. The cycle length averages 11 years but has varied from 7 to 17 years (Fig. 5), with shorter cycle lengths corresponding to a more magnetically-active Sun. A remarkably close agreement was found between the sunspot cycle length and the change in land temperature of the Northern Hemisphere in the period between 1861 and 1989 (Fig. 6). The land temperature of the Northern Hemisphere was used to avoid the lag by several years of air temperatures over the oceans, due to their large heat capacity. This figure covers the period during which greenhouse gas emissions are presumed to have caused a global warming of about 0.6°C. Two features are of particular note: firstly the dip between 1945 and 1970, which cannot be explained by the steadily rising greenhouse gas emissions but seems well-matched to a decrease in the Sun's activity, and secondly the close correspondence between the two curves over this entire period, which would seem to leave little room for an additional greenhouse gas effect.

In the absence of sufficiently sensitive measurements, people suspected that the Sun's irradiance may be fluctuating over the solar cycle. However, from our knowledge of how the Sun produces energy, this would seem difficult. Radiation from the Sun was created in the core and, in a random walk with a mean free path of about 10 cm, has taken about fifty million years to reach the surface. This would smooth out any substantial fluctuations in radiated energy on a timescale significantly less than about a million years. Indeed the steadiness of the Sun's irradiance over a complete sunspot cycle has recently been confirmed by satellite measurements (Fig. 7 [7]). The solar flux is slightly higher at sunspot maximum; although sunspots are cooler and have reduced emission, this is more than compensated by an associated increase in bright areas known as *plages* and *faculae*. The mean irradiance changes by about 0.1 % from sunspot maximum to minimum which, if representative over a longer time interval, is too small (0.3 Wm^{-2}, globally-averaged) to account for the observed changes in the Earth's temperature.

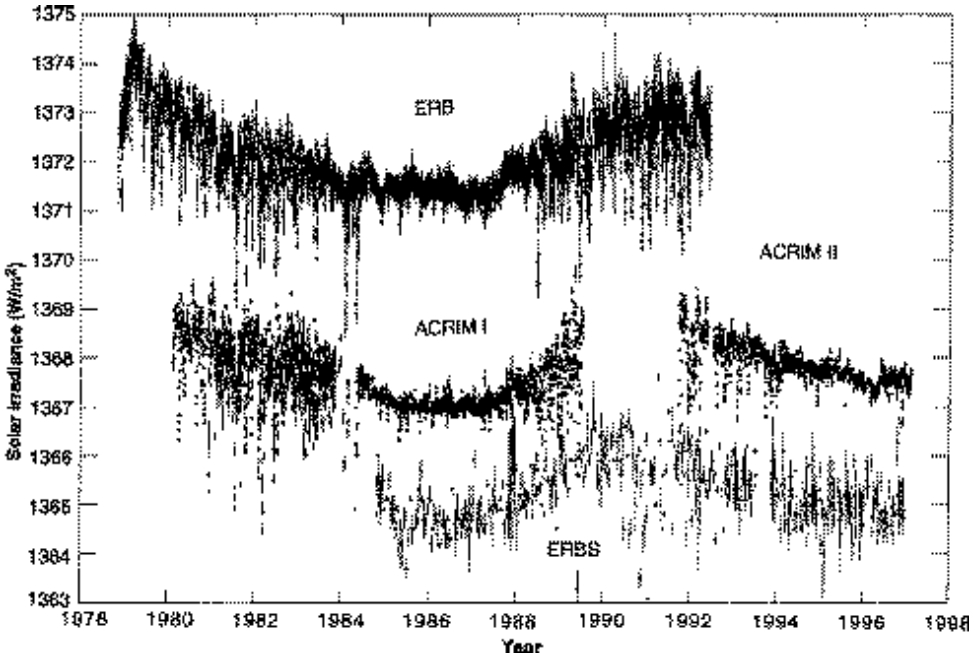

Figure 7: Satellite measurements of the variation of the Sun's irradiance over a 1.5 sunspot cycles, showing daily mean values and uncertainties [7]. Approximately, sunspot maxima occurred during 1980 and 1990, and sunspot minima occurred during 1985–86 and 1996. The rapid fluctuations at the maxima are due to sunspots rotating into the field of view. The data are from the Active Cavity Irradiance Monitor (ACRIM I and II) and from the Nimbus 7 Earth Radiation Budget (ERB) and Earth Radiation Budget Satellite (ERBS) experiments.

2.2 The missing link: cosmic rays?

Experimental observations. It has been recognised for several decades that the cosmic ray flux reaching the Earth is strongly modulated by the solar wind[3] which, in turn, is strongly influenced by the sunspot cycle (Fig. 8). At times of high sunspot activity, the solar wind is stronger and this partially shields the lower-energy galactic cosmic radiation from penetrating the inner solar system and reaching the Earth. In addition, the lower-energy cosmic rays are affected by the geomagnetic field, which they must penetrate to reach the top of the atmosphere. The minimum vertical momentum of primary charged particles at the geomagnetic equator is about 15 GeV/c, decreasing to below 0.1 GeV/c at the geomagnetic poles. The modulation of the cosmic ray flux incident on the Earth's atmosphere at the higher geomagnetic latitudes is as large as 50% between sunspot maxima and minima [8]. It represents one of the largest measurable effects of sunspot activity near the Earth's surface.

But how could cosmic rays affect the Earth's weather? The breakthrough was made by

[3]The solar wind is a continuous outward flow of charged particles (mainly protons and electrons, with 5% helium nuclei) from the plasma of the Sun's corona. The main sources are near the Sun's poles; other important sources include coronal holes and sunspots. The solar wind creates the huge heliosphere of the Sun that extends out to Neptune and beyond. At the Earth's orbit the solar wind has a velocity of 300–800 km s^{-1} ($\beta = 0.001$–0.003) and an intensity of (0.5–5)$\times 10^8$ particles cm^{-2} s^{-1}, generating a magnetic field of about 5×10^{-5} Gauss.

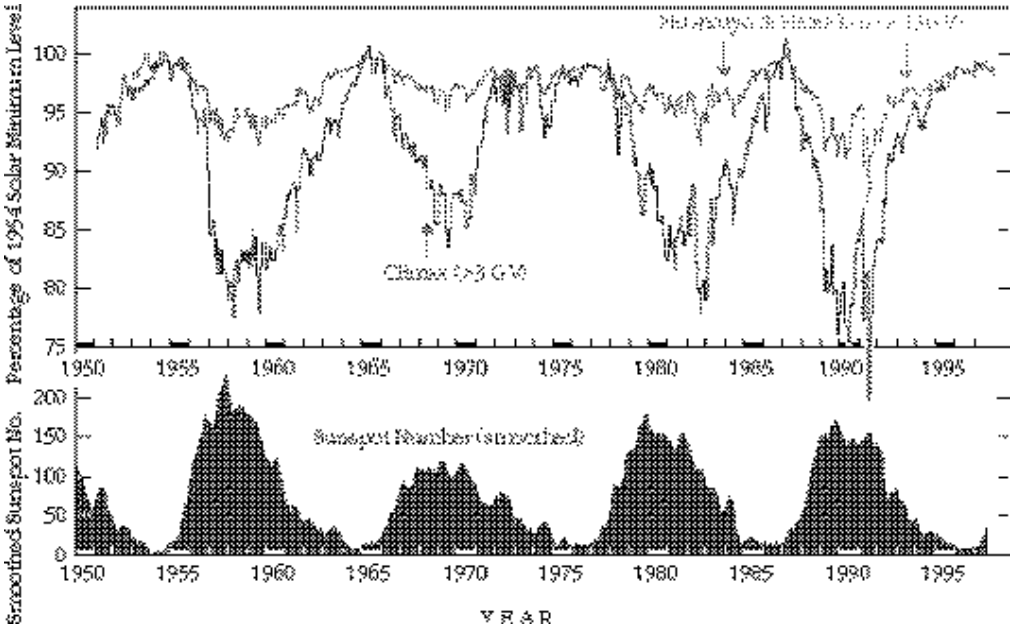

Figure 8: Variation with time of sunspot number and cosmic ray flux, as measured by ground-based neutron counters. The neutron data are from the Univ. Chicago Neutron Monitor Stations at Climax, Colorado (3400 m elevation; 3 GeV primary charged particle cutoff), Huancayo, Peru (3400 m; 13 GeV cutoff) and Haleakala, Hawaii (3030 m; 13 GeV cutoff). The stronger modulation of the cosmic ray flux at higher latitudes (Climax) is due to the lower primary cutoff energy.

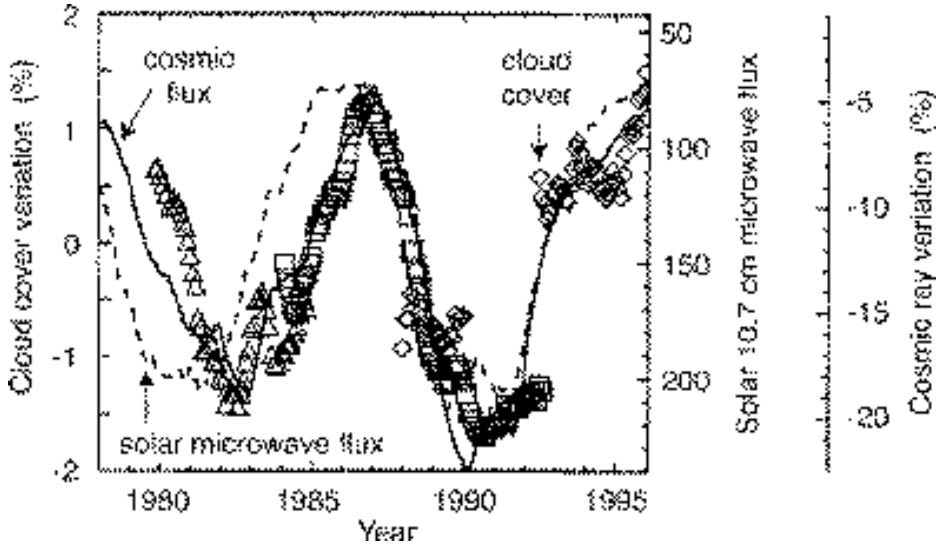

Figure 9: Absolute percentage variation of global cloud cover (data points; left-hand scale) and relative percentage variation of cosmic ray flux (solid curve, normalised to May 1965; right-hand scale) [2, 3]. Also shown is the solar 10.7 cm microwave flux (dashed curve, in units of 10^{-22} $Wm^{-2}Hz^{-1}$; right-hand scale). The cloud data are restricted to oceans; Nimbus 7 (triangles) and DMSP (diamonds) data are for the total Southern Hemisphere over oceans, and ISCCP (squares) data are for oceans with the tropics excluded. The cosmic ray data are neutron measurements from Climax (see Fig. 8). All data are smoothed using a 12-month running mean.

Svensmark and Friis-Christensen in 1997 [2, 3] who showed a striking correlation between global cloud cover and the incident cosmic ray flux (Fig. 9). Moreover, the cloud cover was found to have a poorer correlation with variations in the solar microwave flux (Fig. 9). The latter is known to follow closely variations in the total solar irradiance, soft X-rays and ultraviolet rays. The modulation in cloud cover was found to be more pronounced at higher geomagnetic latitudes, consistent with the reduced shielding effect of the Earth's magnetic field at higher latitudes (see Fig. 8).

Over a sunspot cycle, the absolute variation in global cloud cover is about 3% (equivalent to 4.8% relative fraction), and the variation in the neutron flux is about 15–20% (for a primary charged particle cutoff of 3 GeV). The neutrons are mostly produced by primary hadronic interactions in the first 1–2 λ_{int} of the atmosphere and therefore measure the changes in cosmic ray intensity at altitudes above about 13 km. The primary cosmic radiation is about 80% protons, 15% He nuclei and 5% heavier nuclei. At sea level the most numerous *charged* particles are muons and their fluctuation is less pronounced, about 3% over a solar cycle [8], since they are produced from a stiffer primary spectrum of cosmic radiation, which is therefore less affected by the solar wind.

Fraction of clouds affected by cosmic rays. These data suggest that cosmic radiation is, under suitable atmospheric conditions, either extending cloud lifetimes (for example, by increasing the droplet number density) or inducing some additional cloud formation. The currently-accepted physical processes that affect the production of cloud condensation nuclei [9, 10], including both aerosols and ice particles, do not consider ion-induced effects. The new satellite observations suggest that the ions or radicals produced in the atmosphere by cosmic rays may somehow be affecting the nucleation, growth or activation of atmospheric aerosols, or the creation of ice particles.

It is interesting to estimate the total cloud fraction that may be caused by cosmic rays. It is not yet known at which altitude the cosmic radiation may be affecting clouds, i.e. whether the clouds more closely follow the amplitude modulation of the neutron flux (20%) or of the muon flux (3%). However, making the most conservative assumption, a 20% change in cosmic ray flux causes a 4.8% relative change in cloud cover. If the cloud-forming process is directly proportional to cosmic flux then this suggests about 25% of the Earth's clouds could be affected by cosmic rays. However, if the process is proportional to ion density then the fraction is twice as large, since a 20% increase in cosmic ray flux leads to a 10% increase in equilibrium ion density (see Section 3.2). In summary, a large fraction of the Earth's clouds could be affected by cosmic radiation.

Effect on the Earth's radiation budget. Thin clouds at high and middle altitudes cause a net warming due to an increased trapping of outgoing longwave radiation whereas optically thick clouds produce a net cooling due to a dominant increase in the albedo (reflection) of the incoming shortwave solar radiation. At present there is no indication which clouds may be affected by cosmic rays, so we will assume for the present estimate that all are affected equally. Present estimates from the Earth Radiation Budget Experiment (ERBE) indicate, overall, that clouds reflect more energy than they trap, leading to a net cooling of 28 Wm^{-2} from the mean global cloud cover of 63% (Table 1 [11]). The 4.8% relative variation in cloud cover due to variations of the cosmic ray flux over a solar cycle therefore implies a change in the Earth's radiation budget of 1.3 Wm^{-2} (0.4% of the total

incident solar radiation). This is a significant effect: in the 3-year period 1987–1990, the effect of the reduction in cosmic ray flux was comparable to the total estimated radiative forcing of 1.5 Wm^{-2} from the increase in CO_2 concentration since 1750.

Table 1: Global annual mean forcing due to various types of clouds, from the Earth Radiation Budget Experiment (ERBE) [11]. The sign is defined so that positive forcing increases the net radiation budget of the Earth and leads to a warming; negative forcing decreases the net radiation and causes a cooling.

Parameter		High clouds		Middle clouds		Low clouds	Total
		Thin	Thick	Thin	Thick	All	
Global fraction	(%)	10.1	8.6	10.7	7.3	26.6	63.3
Forcing (relative to clear sky):							
Albedo (SW radiation)	(Wm^{-2})	-4.1	-15.6	-3.7	-9.9	-20.2	-53.5
Outgoing LW radiation	(Wm^{-2})	6.5	8.6	4.8	2.4	3.5	25.8
Net forcing	(Wm^{-2})	2.4	-7.0	1.1	-7.5	-16.7	-27.7

Open questions. Despite the observation of Svensmark and Friis-Christensen (Fig. 9), a direct link between cosmic rays and cloud formation has not been unambiguously established. The satellite data are a composite of several datasets which are subject to inter-calibration uncertainties. Furthermore the data are spatially and temporally selective - they are restricted to oceans and exclude the tropics and polar regions, and they are largely daytime only.

It has been argued that the single sunspot cycle for which there are reliable satellite measurements is insufficient to demonstrate a clear connection and that several more cycles (each of course requiring 11 years) are needed. Even if this extended study were to confirm the correlation between the sunspot cycle and cloud cover, it may not prove the missing link is cosmic rays. While cosmic rays certainly vary with the sunspot cycle, other factors that change during the cycle may be affecting clouds, quite independently of cosmic rays. For example, the cause may be variations of the solar ultra-violet (UV) radiation. Although the total irradiance of the Sun varies by only 0.1 % over the solar cycle, the variation is more pronounced in the UV. Wavelengths below 320 nm, which account for only about 2% of the total solar irradiance, vary by about 5% (200–320 nm) to 50% (100–150 nm), or even more at shorter wavelengths [15]. The UV radiation is absorbed by ozone high in the stratosphere which warms as a result. This has the potential to influence large scale tropospheric dynamics and hence, perhaps, cloudiness.

Finally, the evidence of increased variations in cloud production at higher latitudes, while consistent with the cosmic ray explanation, could simply be due to the variations with latitude of temperature, air circulation, aerosols and other atmospheric conditions that affect cloud formation.

2.3 History of cosmic rays and climate change

If the periodic 11-year cycles of the sunspots and the associated cosmic ray flux were the end of the story, then it would be of limited concern since there would be no resultant long-term change in the Earth's weather but simply another cyclic "seasonal" change (albeit with a period of 11 years). However there is clear evidence of longer-term and unexplained changes both in the Sun and in the Earth's magnetosphere and these, in turn, seem to have had long-term effects on the Earth's climate.

2.3.1 Global warming during the present century

Over the course of this century the cosmic ray flux has been steadily decreasing; it is weaker today at its *maximum* during the sunspot cycle than it was at its *minimum* around 1900. This has been revealed by analysis of the ^{10}Be concentration in a Greenland ice core (Fig. 10 [12]). Beryllium-10 is produced in the atmosphere by cosmic rays and, despite a lower production rate than ^{14}C (Section 2.3.2) by about a factor 100 (3.5×10^{-2} atoms cm^{-2}s^{-1}), it has the advantages of settling out relatively rapidly ($\sim$ 2 years) and of a long half-life, 1.51×10^6 years. A systematic decrease in the cosmic ray flux of the magnitude indicated by the ^{10}Be data would have caused a reduction in cloud cover and consequent warming of the Earth, sufficient to account for a large part of the observed rise of 0.6°C in global temperatures over this century which is presently attributed to anthropogenic greenhouse gases.

The cause of this systematic decrease of the cosmic flux has been a strengthening of the solar wind over this century. This is revealed in measurements of the so-called *aa geomagnetic index* of short-term (up to 3-hour) variations in the geomagnetic field at the Earth's surface [13, 14], which is affected by the interactions of the solar wind with the Earth's magnetosphere (Fig. 11). With this hindsight, the previous observation by Friis-Christensen and Lassen that the sunspot *cycle length* is closely correlated with global temperatures (Fig. 6) can now perhaps be understood: the sunspot cycle length is a direct measure of the strength of the solar wind and a better measure than the sunspot number itself. Shorter sunspot cycles correspond to a stronger solar wind and therefore to decreased cosmic flux, decreased cloud cover and increased temperatures.

Although a comparison of global temperatures with direct measurements of cosmic rays can only be made since 1937, when systematic measurements of charged cosmic rays began with electronic detectors, the two are indeed found to correlate well (Fig. 12 [3]).

2.3.2 Climatic change over the past millennium

The observations of a correlation between the Sun's activity, cosmic rays and the Earth's climate may be extended to earlier times with ^{14}C data. This isotope is continuously formed in the atmosphere by low energy neutrons from cosmic radiation at a rate of about 2.5 atoms cm^{-2}s^{-1}, in the reaction:

$$^{14}\mathrm{N} + \mathrm{n} \rightarrow {}^{14}\mathrm{C} + \mathrm{p}$$

The ^{14}C is rapidly oxidised to form $^{14}CO_2$ and then decays by β^- emission with a half life of (5730 ± 40) years. The turnover time of CO_2 in the atmosphere is quite short, about 4 years, mostly by absorption in the oceans and assimilation in living plants. However,

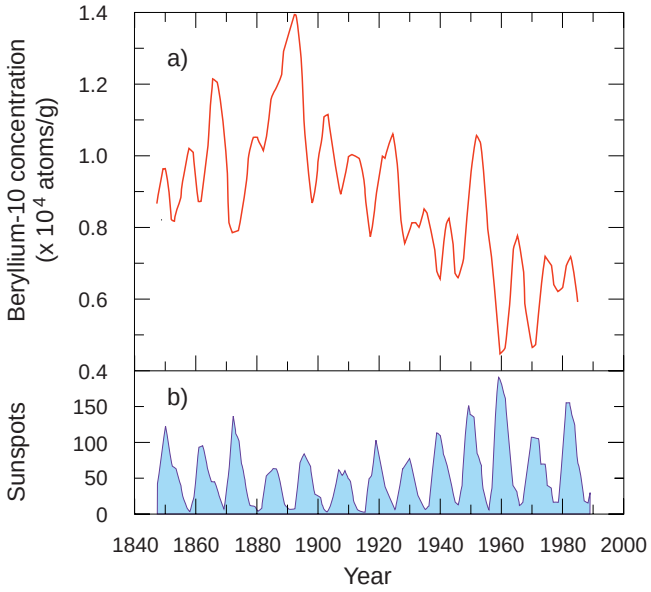

Figure 10: a) Concentration of ^{10}Be in a 300 m ice core from Greenland over the last 150 years [12]. The data are smoothed by an approximately 10 year running mean and have been shifted earlier by 2 years to account for settling time. b) The sunspot cycle over the same period, which shows a negative correlation with the short-term ($\sim$ 11 year) modulation of the ^{10}Be concentration.

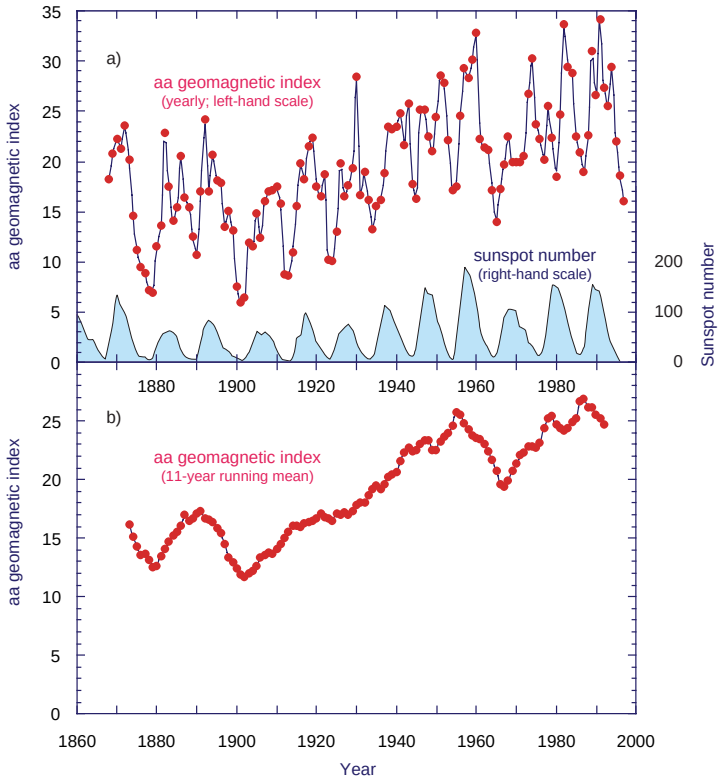

Figure 11: Variation of the aa geomagnetic index over the last 130 years: a) yearly measurements and b) data smoothed by an 11-year running mean. The sunspot cycle over the same period is indicated in the upper figure and shows a positive correlation with the short-term ($\sim$ 11 year) modulation of the aa geomagnetic index.

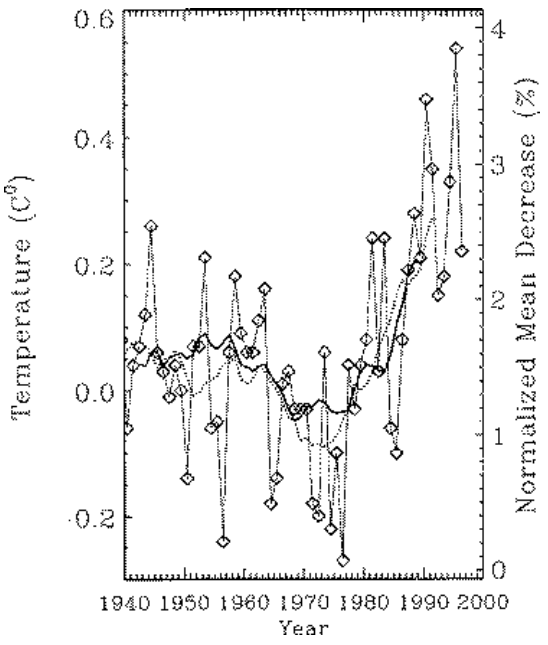

Figure 12: Northern hemisphere mean temperature (dotted line; left-hand scale) and charged cosmic ray flux (thick solid line; right-hand scale) since 1940 [3]. Both curves are smoothed by an 11-year average. The diamonds show the annual temperatures, before smoothing.

recirculation from the oceans has a smoothing effect such that changes in the ^{14}C fraction on timescales less than a few decades are smoothed out. Plant material originally contains the prevailing atmospheric fraction of ^{14}C and subsequently, since the material is not recycled into the atmosphere, the fraction decreases with the characteristic half life of ^{14}C.

By analysing the ^{14}C content in the rings of long-lived trees such the Californian bristlecone pine, a year-by-year record has been assembled of the cosmic ray flux on Earth over the past several thousand years. The data for the last 1000 years are shown in Fig. 13 [5]. (In this the following two figures, the vertical axis is oriented so that warmer temperatures point upwards.) It is interesting to note that the periods where the ^{14}C deviation exceeds 10 parts per mil correspond to recorded climatic anomalies: a) 1100–1250, the so-called Medieval Warm period, b) 1300–1360, the Wolf maximum, c) 1460–1550, the Spörer minimum, and d) 1645–1715, the Maunder minimum. The warm period that lasted until about 1400 enabled the Vikings to colonise Greenland and wine to be made from grapes grown in England. It was followed by a period of about 400 years during which the glaciers advanced and cooler, harsher conditions prevailed in most parts of the world.

The Maunder Minimum, when there was an almost complete absence of sunspots, would have corresponded to a high cosmic ray flux on Earth and therefore an increased cloudiness. This provides a consistent explanation for the exceptionally cold weather of this period. Indeed, in every case the excess (c–d) or lack (a–b) of ^{14}C is consistent with the observation of a higher cosmic ray flux leading to more clouds and cooler temperatures, and vice versa.

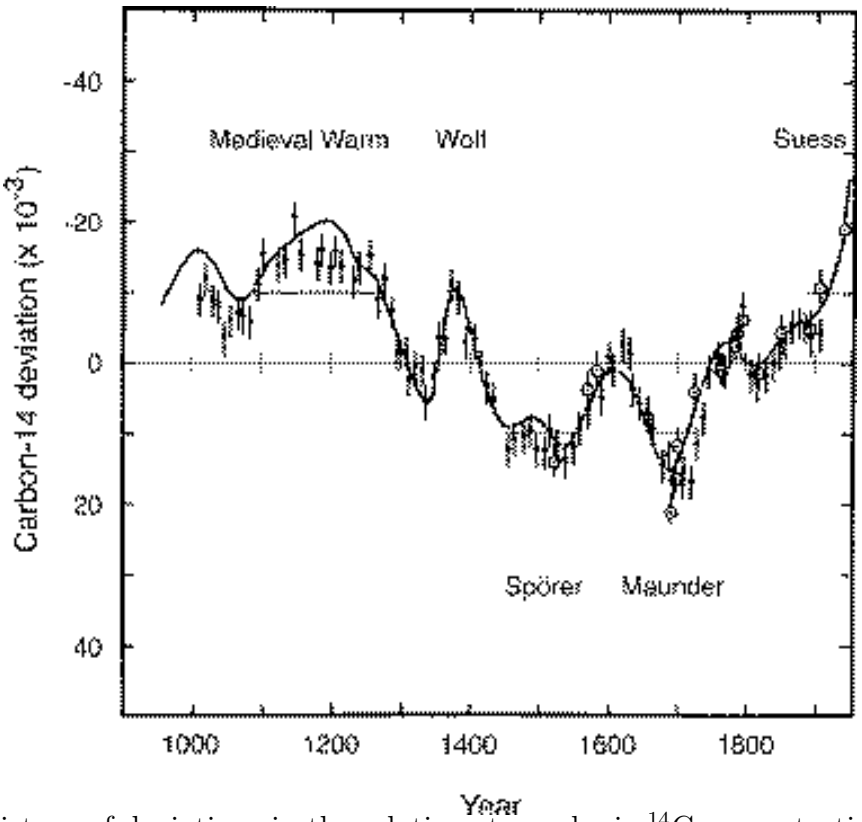

Figure 13: History of deviations in the relative atmospheric ^{14}C concentration from tree-ring analyses for the last millennium [16]. The data points (dots and open circles) are two independent high-precision measurements. The solid line represents a combined fit to a large number of other measurements of medium precision. Periods where the deviation of the data points exceeds 10 parts per mil are indicated. The first four coincide with recorded climatic anomalies. The sharp negative ^{14}C deviation during the present century is the Suess effect, due to the burning of ^{14}C-depleted fossil fuels.

These data provide evidence for significant temperature anomalies over the last millennium that coincided with variations of the cosmic ray intensity. Furthermore they show that the Earth has experienced several extended warm and cold spells over the last 1000 years—with climate swings comparable to the current "anomaly"—whose origin certainly cannot be due to anthropogenic greenhouse gases. Whatever caused those earlier spells could well be at work today.

2.3.3 Climatic change since before the last ice age

The ^{14}C record has been extended even earlier; the last 10,000 years is shown in Fig. 14 [17] and the last 30,000 years in Fig. 15 [18]). There are several important conclusions to be drawn from these data. Firstly, there have been very large systematic changes in the cosmic ray flux over this period, namely about 40% (where a systematic shift of only 1% is known to be associated with a significant climate change, as seen in Fig. 13). Secondly, the ending of the last great ice age, 17,000–10,000 years ago, coincided with a sharp decrease of the ^{14}C fraction (Fig. 15). Part of this is due to the reduction in ice cover and the higher temperatures, thereby increasing the circulation of ^{14}C-depleted

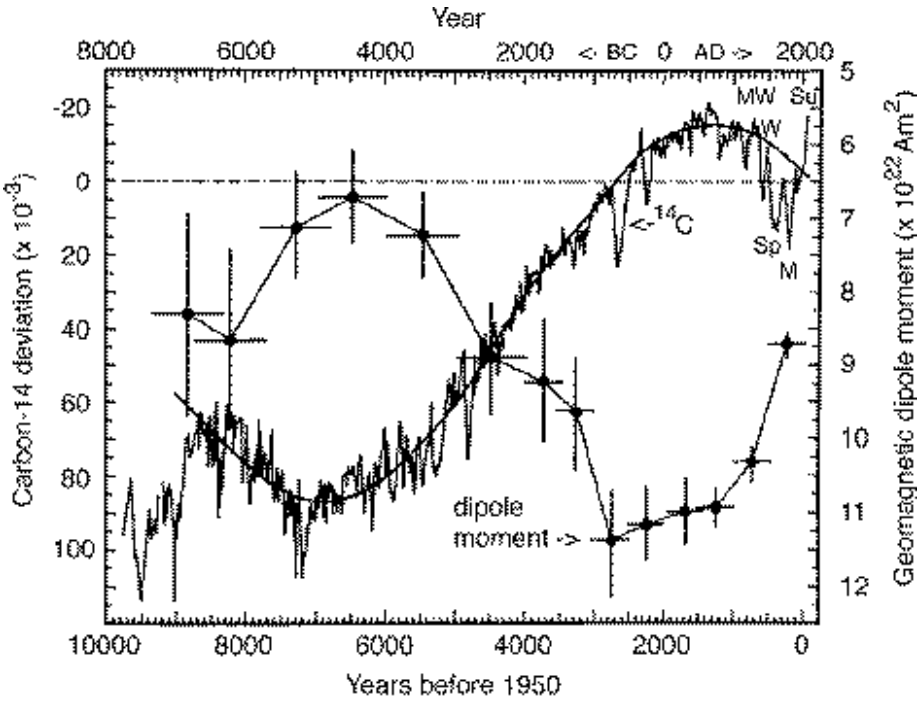

Figure 14: History of deviations of the atmospheric ^{14}C concentration over the last ten millennia relative to the 1850 value (left-hand scale) [16]. The Medieval Warm (MW), Wolf maximum (W), Spörer minimum (Sp), Maunder minimum (M) and Suess deviation (Su) are indicated. The data points show the Earth's magnetic dipole moment over the same period (right-hand scale) [16].

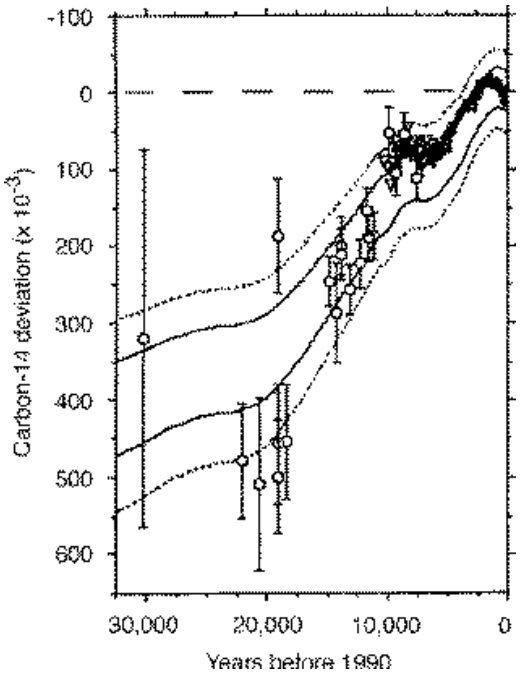

Figure 15: Variation of the atmospheric ^{14}C over the last 30 millennia [18]. The two sets of lines correspond to theoretical expectations based on changes of the Earth's magnetic field; the solid lines assume ±5% of the present-day dipole and the dotted lines, 10%.

CO_2 from the oceans. An estimated decrease in the atmospheric ^{14}C fraction from these effects is 10% [16]. The measured change (Fig. 15) is substantially larger, suggesting that this period may have coincided with a decrease of the cosmic flux.

These large changes in the cosmic ray flux have been caused by changes in the Earth's magnetic field[4] and its associated shielding effect. The geomagnetic field is independently measured and found to closely track the cosmic ray flux, as shown in Figs. 14 and 15. This record of changes in the cosmic ray flux, and the expected effects on global climate, correlate with the climate records derived from analyses of cores drilled in the Greenland ice sheet. However it is important to keep in mind that, even if cosmic rays can indeed affect cloud formation, it would also require the existence of suitable atmospheric conditions (humidity, aerosol content, etc.) and that these were probably quite different during the glacials.

Finally, on an even longer timescale, it is known that the Earth's magnetic field *reverses* periodically (approximately every million years). During these reversals—which may take place fairly rapidly over periods of less than 1000 years—the Earth's field diminishes to zero and then re-establishes itself with the opposite polarity. At such times the Earth will be subjected to far higher cosmic ray fluxes and the temperatures will be greatly reduced. This may perhaps be a factor contributing to the extinction of the dinosaurs 65 million years ago, which coincided with a geomagnetic reversal.

2.4 Conclusions

In summary, there are two main conclusions to be drawn on the connection between cosmic rays and climate change. Firstly, the pattern of systematic change in the global climate over the past several thousand years follows the observed changes in the cosmic ray flux over the same period; and it is consistent with the explanation that a high cosmic ray flux corresponds to more clouds and a cooler climate, and vice versa. Furthermore, the rise of about 0.6°C in global temperatures over the last 100 years is consistent in magnitude and time dependence with the observed changes in cosmic ray flux—and thereby cloud cover—over the same period. A clear and compelling case exists for further study of the effect of cosmic rays on cloud formation and climate change—especially in order to improve model calculations of the residual effects due to greenhouse gases from the burning of fossil fuels.

Secondly, since the cosmic ray flux is controlled both by the Sun's magnetic activity (solar wind) and by the Earth's magnetic field, it may eventually be possible to make long-term (10–1,000 year) predictions of changes in the Earth's climate by detailed measurements and a deeper understanding of the "magnetic climate" of the Sun and Earth and its effect on the cosmic ray flux. In this regard, it will be necessary to understand how the Sun changes its magnetic activity and to understand the progression of the Earth's magnetic moment. Perhaps even the longer-term Milankovitch cycles are partly influencing the global climate through geomagnetic effects; the Earth's magnetic field is due to electric currents flowing in the liquid core and in the magnetosphere, and these may have been influenced by the periodic gravitational motions of the Milankovitch cycles.

[4]The Earth's field is presently weakening (Fig. 14), which may indicate a cooling period ahead.

3 Cloud formation by charged particles

Cloud droplets in the troposphere[5] form on suitable aerosols above about 100 nm size known as cloud condensation nuclei (CCN) [9, 10]. The new satellite observations suggest that the ions or radicals produced in the atmosphere by cosmic rays may somehow be affecting the nucleation, growth or activation of atmospheric aerosols, or affecting the creation of ice particles. An increase of CCN concentration could lead to increased droplet number concentration, smaller droplet size, less precipitation and therefore longer cloud lifetime. If cosmic rays can affect ice nuclei then this would also potentially have a strong influence on clouds since the freezing of supercooled water droplets reduces their vapour pressure and allows their growth at the expense of neighbouring liquid droplets.

A microphysical explanation of cloud formation in the presence of ionising radiation is presently lacking. In fact there has been very little research on this mechanism and present studies do not consider it [10]. Some experiments with highly charged droplets (10^{-14}–10^{-11} C) have, however, shown that they are 10–100 times more efficient at capturing aerosols than uncharged droplets [19].

3.1 Droplet formation in a conventional cloud chamber

Certain aspects of how droplets are induced by ionising radiation are known from the development of cloud chambers, but these largely concern high supersaturations of water vapour and rapid growth rates. The principle of operation of a cloud chamber [20] can be understood from Fig. 16 which shows the water vapour pressure equilibrium curves for small droplets:

$$\log_e\left(\frac{p}{p_0}\right) = \frac{M}{RT\rho}\left[\frac{2\gamma}{r} - \left(\frac{Q^2e^2}{4\pi\epsilon_0 r^2}\cdot\frac{1}{8\pi r^2}\right)\right],$$

where p is the vapour pressure, p_0 the saturated vapour pressure at a plane water surface, R the gas constant, T the absolute temperature, γ the surface tension, M the molecular weight, ρ the density, ϵ_0 the permittivity of free space and r the radius of the droplet. The curves divide an upper region of vapour pressure in which water droplets grow by condensation (e.g. droplet D_1) from a lower region where they shrink by evaporation (e.g. D_2). If a droplet carries an electric charge Qe then its vapour pressure is reduced by increased attraction of the polar water molecules. The growth region is therefore larger (Fig. 16a) and, in particular, for supersaturations above about 5, *all* charged droplets will grow and reach visible size (e.g. D_3). The actual starting point for a droplet is not known. However, to set the minimum scale we can estimate the volume occupied by a single water molecule as $\frac{4}{3}\pi r^3 = \frac{M/\rho}{N_A}$, where N_A is Avogadro's constant. This indicates the effective radius of one water molecule is $r \sim 0.2$ nm; and a droplet of radius 0.5 nm contains about 15 molecules.

[5]The troposphere is the lowest level of the atmosphere and the region where there is enough water vapour and vertical mixing for clouds to form under suitable conditions. The depth of the troposphere is about 6–8 km at the poles, extending to about 17 km over the equatorial regions; it contains about 75% of the mass of the atmosphere. There is an overall adiabatic lapse rate of temperature in the troposphere by between 6°C (moist air) and 10°C (dry air) per km altitude, reaching a minimum of about -60°C at the boundary with the stratosphere (the tropopause). The stratosphere, which extends up to about 50 km, has a temperature that slowly rises with altitude. This leads to very little turbulence and vertical mixing and, in consequence, it contains warm dry air that is largely free of clouds.

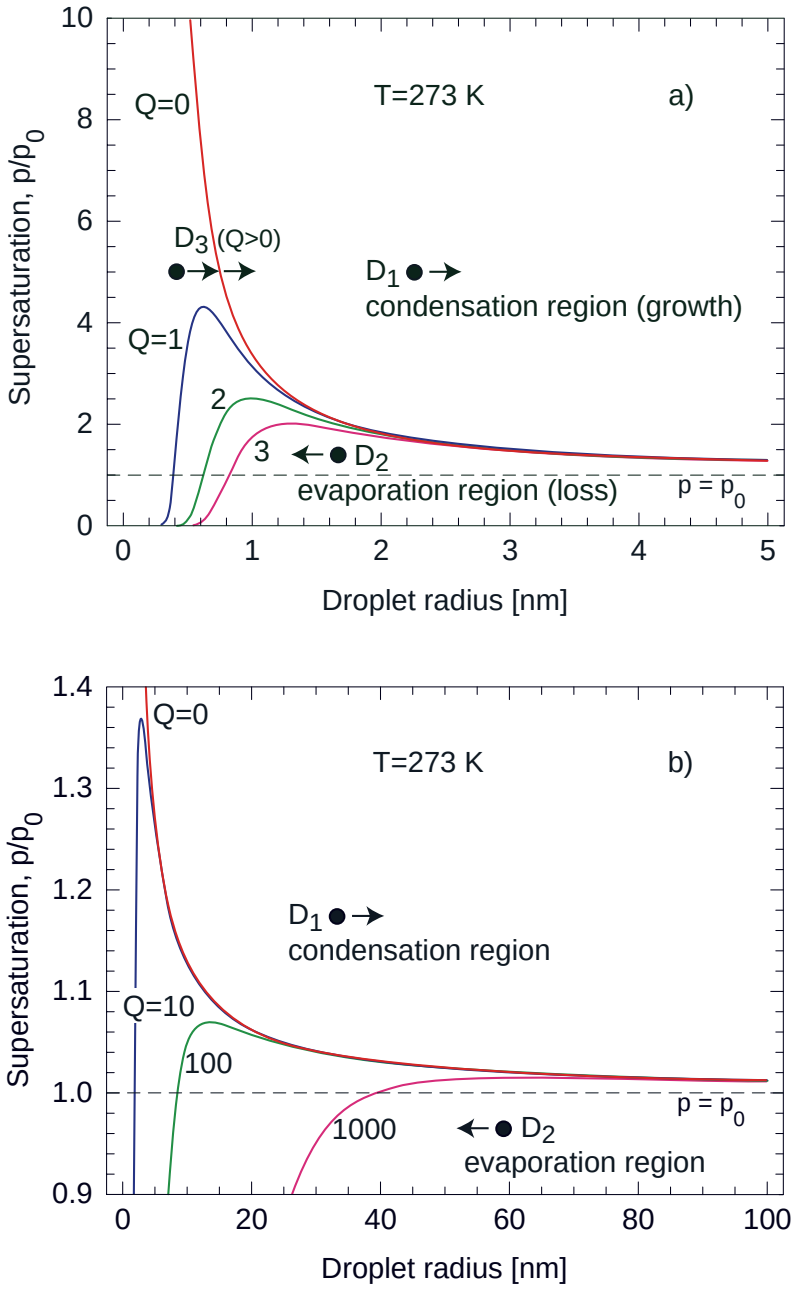

Figure 16: Formation of charged droplets at 0°C and various supersaturations of water vapour, for droplet radii less than a) 5 μm and b) 100 μm. The curves are labelled according to the droplet electronic charge, Qe. The saturated vapour pressure, p_0, corresponds to equilibrium with a plane water surface. Droplets formed in the region above the curves will grow (condensation region) and those below will shrink (evaporation region).

The necessary supersaturation in a cloud chamber is generated by fast adiabatic expansion. For an ideal gas and an adiabatic expansion,

$$\begin{aligned} P_1 V_1^{\gamma} &= P_2 V_2^{\gamma}, \quad \text{and} \\ T_1 V_1^{\gamma-1} &= T_2 V_2^{\gamma-1}, \end{aligned}$$

where γ is the ratio of specific heats C_P/C_V (about 1.40 for air and saturated water vapour). For example, an expansion ratio $V_2/V_1 = 1.3$ results in a temperature drop of about 30°C and a supersaturation of 4.8. Under these conditions, all droplets with $Q \geq 1$ will grow to diameters of several tens of micrometres in $\lesssim 0.2$ s.

The curves of Fig. 16a) indicate how the presence of a small charge facilitates droplet formation and growth at high supersaturations, above about 2. The maximum supersaturations in the troposphere are typically less than one per cent above unity which, if this were the only mechanism involved, would require large droplet charges for stable growth, as indicated in Fig. 16b). Therefore if ionising radiation is indeed inducing additional cloud formation, it must be somehow affecting the aerosols or ice nuclei that efficiently seed clouds in the atmosphere.

3.2 Ions and droplets in the atmosphere

To provide input for the design requirements of the CLOUD detector, it is useful to estimate some characteristics of cosmic-ray ionisation and water droplets in the troposphere. Some representative parameters at the upper and lower boundaries of the troposphere are summarised in Table 2. These regions are well below the ionosphere—which starts above the stratosphere at about 80 km altitude—where atoms and molecules are readily ionised by solar UV and X-ray photons.

Table 2: Approximate characteristics of cosmic rays near the top of the troposphere (10 km altitude) and at sea level. The maximum and minimum charged cosmic ray fluxes, ϕ, correspond to the sunspot cycle variation at geomagnetic latitudes $\gtrsim 40^{\circ}$ and for energies $\gtrsim 0.1$ GeV. The # ion pairs cm^{-1}, n_{ip}, are the ionising track densities for minimum ionising particles in air.

Atmospheric characteristics					Cosmic ray characteristics			
Alt.	Atmos. depth	Pressure	Density	Mean. temp.	Chd. flux, ϕ [m^{-2}sr^{-1}s^{-1}]		Ion pairs /cm, n_{ip}	Recombination coefficient, α
[km]	[λ_{int}]	[kN m^{-2}]	[kg m^{-3}]	[°C]	Max.	Min.	[cm^{-1}]	[m^{3}s^{-1}]
10	3.0	26.4	0.41	-50	850	750	23	0.64×10^{-12}
0	11.5	101.3	1.22	15	100	97	68	1.72×10^{-12}

The rate of ion-pair production by cosmic rays, $r_{ip} = \phi\ \Omega\ (100\ n_{ip})$. From Table 2 this rate is about $2{\times}10^6$ m^{-3}s^{-1} at sea level and 10^7 m^{-3}s^{-1} at 10 km altitude. Once created, the charged particles will recombine. The electrons are rapidly captured by electronegative gases, which become negatively charged as a result. For example, at 0°C

and atmospheric pressure, the mean electron attachment time is 190 ns in O_2 and 140 ns in H_2O vapour.

The ion mobility is far smaller and consequently so also is the ion recombination rate:

$$\frac{dn_+}{dt} = \frac{dn_-}{dt} = -\alpha\, n_-\, n_+, \tag{1}$$

where n_+ and n_- [m^{-3}] are the positive and negative ion densities and α is the recombination coefficient. Equilibrium is reached when the ion production and recombination rates are equal, i.e. when $r_{ip} = \alpha\, n_+\, n_-$. Assuming $n_+ \sim n_-$ implies the equilibrium ion density, $n_{eq} = \sqrt{r_{ip}/\alpha}$. From Table 2, this indicates n_{eq} is about 10^9 m^{-3} at sea level and 4×10^9 m^{-3} at 10 km.[6] These estimates apply to still air without aerosols, water droplets, etc. The equilibrium ion density $n_{eq} \propto \sqrt{\phi}$ so that, for example, the ∼12% change in cosmic ray flux at 10 km altitude over a sunspot cycle produces ∼ 6% change in the ion density.

From equation 1, the lifetime of an ion is $\tau = 1/(\alpha\, n_{eq})$. This implies ion lifetimes in the troposphere of about 6–9 min. In still air, the ions drift vertically in the electric field created by the negatively-charged Earth and the positively-charged ionosphere. The field strength is $E \sim 100$ V/m at sea level, producing an ion drift velocity of about 0.022 m s^{-1}. This results in an ion drift distance of about 12 m before recombination.

In the CLOUD detector, in the absence of a drift field, the ions will diffuse a projected distance $\sigma_x = \sqrt{2Dt}$ in a time t, where D is the diffusion coefficient. For water vapour, $D = 1.6 \times 10^{-6}$ $m^2 s^{-1}$ at conditions corresponding to sea level and 4.1×10^{-6} $m^2 s^{-1}$ at those corresponding to 10 km altitude, indicating ion diffusion distances of 4–6 cm before recombination.

In order to be sensitive to long growth times in CLOUD, the droplets must not be removed by gravitational fall before observation. This sets a maximum droplet size for studying long growth times, which can be estimated as follows. Stoke's formula for the viscous force F on a sphere of radius r moving at a velocity v is

$$F = -6\pi\eta r v, \tag{2}$$

where η is the dynamic viscosity (1.7×10^{-5} Pa s for air at 0°C). This indicates a terminal velocity $v_o = (2r^2\rho g)/(9\eta)$, or v_o [μm s^{-1}] = 130 r^2 [μm^2]. A droplet of radius 1 μm therefore has a terminal velocity 130 μm s^{-1} and falls by about 8 cm during a time of 10 min.

Very small droplets will be suspended by Brownian motion. We can estimate their maximum size as follows. The projected Brownian displacement is $\sigma_x = \sqrt{2Dt}$, where $D = \mu kT$, and k is the Boltzmann constant. The mobility is $\mu = v_{drift}/F = 1/(6\pi\eta r)$ (from equation 2), where F is the force causing the drift. Substituting gives the rms projected displacement of a droplet due to Brownian motion, $\sigma_x = \sqrt{(kTt)/(3\pi\eta r)}$. Brownian motion will dominate over gravitational fall when the projected Brownian displacement is about equal to the droplet radius r in the time the droplet would have taken to fall a distance r. This indicates that Brownian displacement is comparable to gravitational displacement at a droplet radius of about 0.7 μm, and below this value droplets will remain suspended for extended periods.

[6]For comparison, the droplet density in clouds is 10^7–10^8 m^{-3} over oceans and 10^8–10^9 m^{-3} over land.

In summary, in order to allow for the possibility of long formation times in the atmosphere, the CLOUD detector should have the capability to observe droplet growth over periods of up to about 10 min, i.e. comparable to the ion lifetime, and the dimensions of the chamber should allow for a fiducial volume that is approximately 10 cm away from any boundary. This indicates a chamber dimension of about $50 \times 50 \times 50$ cm^3 is appropriate.

4 The CLOUD experiment

The basic purpose of the CLOUD detector (Fig. 17) is to confirm, or otherwise, a direct link between cosmic rays and cloud formation by measuring droplet formation in a controlled test-beam environment. The CLOUD detector is essentially a cloud chamber that is designed to duplicate the gases, water vapour, aerosols and temperature/pressure conditions found in the Earth's troposphere.

Since the microphysical mechanisms responsible for cloud formation by cosmic rays are poorly understood, it is necessary for the experimental tests to cover a broad range of variables and conditions. For instance, it is not yet even known at which *altitude* (i.e. temperature and pressure conditions) the clouds are being formed. Also, since the maximum water vapour supersaturation in the troposphere is only about one per cent, droplet growth times may be quite long, as discussed in the previous section. The combined effects of ionisation and aerosols/ice particles is probably important (Section 3). The ionisation of *existing* water droplets by charged particles requires study; charged droplets have a lower vapour pressure and will therefore grow at the expense of uncharged droplets. It is important to measure the sensitivity to a range of track ionisation densities, dE/dx, and ion pair concentrations that duplicates those of cosmic rays. This indicates the need for beam particles ranging from protons to heavy ions. Finally, an investigation should be made of the possibility that droplets are formed in relatively "rare events", such as very highly charged ions or droplets, perhaps due to heavy nuclei.

Cloud chamber data under these conditions have never been previously obtained. Although C.T.R. Wilson's cloud chamber[7] was extensively developed in the first half of this century, it was optimised for experimental particle physics and operated under conditions far removed from those of the troposphere.

4.1 Detector

The CLOUD detector (Fig. 17) comprises the following main components:

- A temperature-controlled cloud chamber that can be operated in the temperature range -60°C to 30°C and at pressures from a vacuum to 1.5 atm. The upper pressure limit is to allow for adiabatic expansions down to a final pressure of 1 atm. An electrode structure (field cage) in the cloud chamber provides a simple clearing field for measurements with low residual ionisation.

[7]It is interesting to note that C.T.R. Wilson had the inspiration for the cloud chamber while observing meteorological phenomena on the mountain of Ben Nevis in 1894. (The phenomena were not particle tracks, however, but "coronas" around the Sun and glories, where the Sun glows around shadows in the mist.)

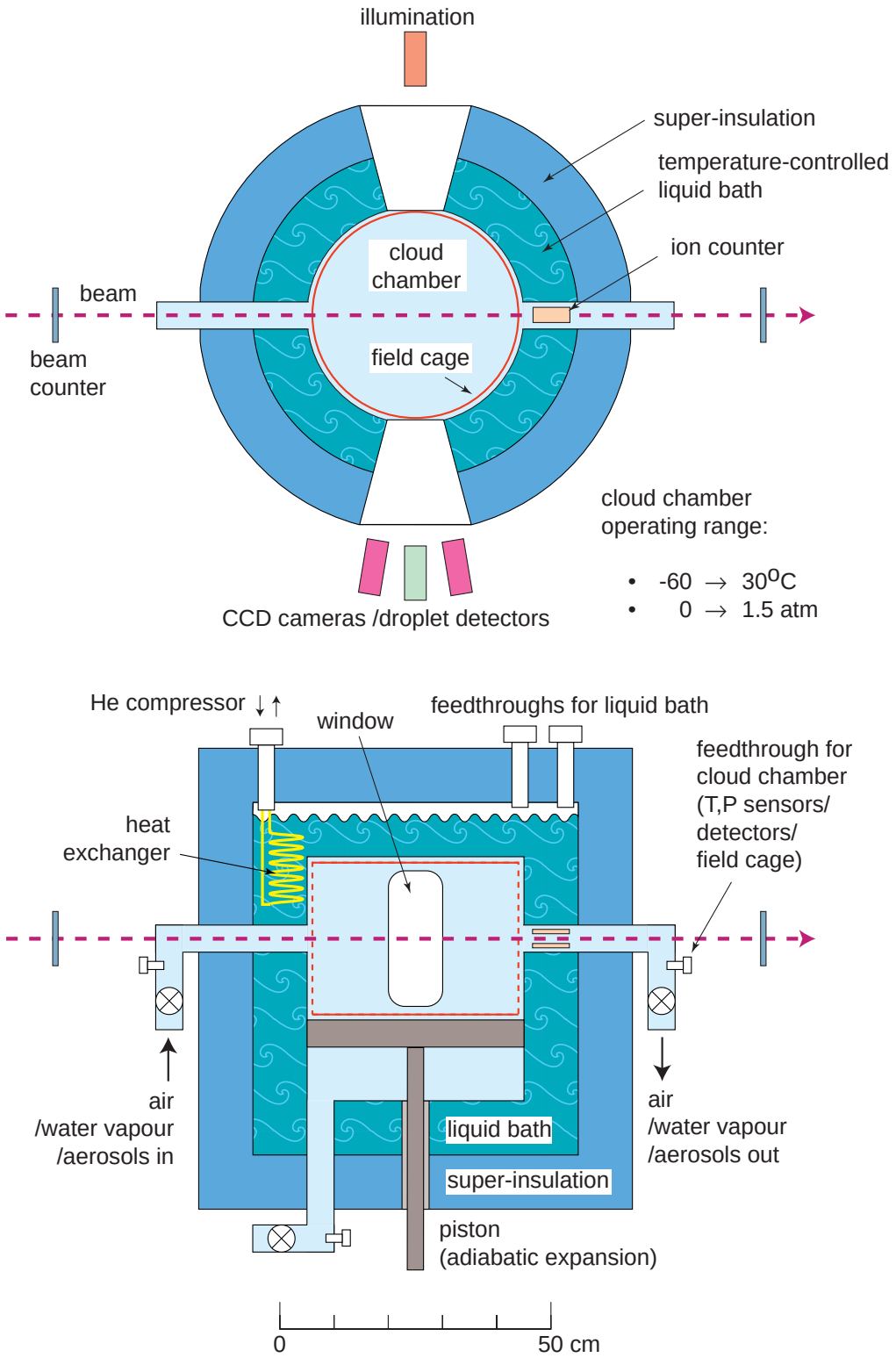

Figure 17: Schematic diagram of the CLOUD chamber.

- A surrounding liquid bath enclosed by super-insulation to provide stable and precise temperature conditions for the cloud chamber. A temperature stability of about 0.01 K is required since this is equivalent to a change of water vapour supersaturation by about 0.05%. The investigation of long growth times for the droplets requires that the operating conditions be held steady for long periods. The temperature is adjusted by heat-exchange coils immersed in a suitable liquid coolant in the bath and connected to a He compressor. The temperature of the circulating He is controlled by temperature monitors immersed in the coolant.

- A piston to provide adiabatic expansions for investigating rapid droplet growth times. Small piston expansions and compressions also provide a technique for fine control of the water vapour supersaturation in the cloud chamber.

- An optical system comprising illumination and stereo microscope cameras (recuperated from old bubble chamber equipment) which can be operated with film or CCD readout. The latter is to allow direct digitization of the data for analysis. The illumination and optical system must be capable of detecting and measuring water droplets of sizes down to a minimum of about 0.5 μm, i.e. the smallest that can scatter light and therefore constitute a cloud. The beam pipe connecting to the cloud chamber is equipped with further detectors to measure the ion/aerosol concentration, size distribution and charge.

- Temperature and pressure monitors.

- A gas system providing air with adjustable amounts of water vapour and aerosols. A mass spectrometer is required for physical and chemical analysis of the incoming and outgoing gas/aerosol mixture.

- A scintillation counter hodoscope to measure the incident beam. The beam must be spread over a large area to simulate the quasi-uniform cosmic radiation.

- A DAQ system.

4.2 Experimental goals

The goals of the proposed study are threefold:

1. **Measurements of water droplet (cloud) formation by ionising radiation**, according to the following variables:

    - Temperature and pressure conditions.
    - Supersaturation of water vapour.
    - Presence of aerosols and trace condensable vapours.
    - Presence of frozen droplets.
    - Presence of existing water droplets.
    - Particle flux and ionisation density (p, heavy ions...).
    - Time for droplet growth.

2. **Understanding of the microphysical processes** involved in cloud formation by ionising radiation. This will involve Monte Carlo simulation of the processes and a comparison with the CLOUD results.

3. **Estimation of the global cloud cover** due to cosmic rays, using atmospheric data recorded by satellite experiments.

5 Conclusions

The observation of an apparent connection between cosmic rays and global climate offers a unique opportunity for particle physics to make a major contribution to the problem of global warming—at a relatively modest cost. The proposed CLOUD experiment will unambiguously confirm, or otherwise, a direct link between cosmic radiation and cloud formation, and allow a quantitative understanding of the physical processes involved. This, in turn, would provide an unambiguous and physically explicable connection between solar and climatic variability—representing a great advance in the understanding of the relationship between the Earth and its star.

Although this experiment primarily addresses atmospheric science, it is clearly in the domain of particle physics and of CERN's expertise and experimental facilities. The CLOUD experiment will have the immediate impact of potentially resolving one of the important unknown effects that may have so far prevented reliable calculations of global warming from greenhouse gases—an issue of profound economic and social importance to the world. Furthermore, if the link is confirmed, then it may eventually become possible to make long-term predictions of systematic changes in the Earth's climate, by monitoring and predicting the evolution of the cosmic ray flux and the "geomagnetic climate" of the Sun and Earth that modulates its intensity.

Acknowledgements

I would like to thank Nigel Calder for an inspiring seminar [21] he presented on this subject at CERN, and also thank Horst Wachsmuth who organised the seminar. I would also like to acknowledge advice from Dietrich Schinzel on the temperature control of the CLOUD detector.

References

[1] Intergovernmental Panel on Climate Change (IPCC), *Climate change 1995: the science of climate change*, eds. J.T. Houghton et al., WMO and UNEP, Cambridge University Press, Cambridge (1996).

[2] H. Svensmark and E. Friis-Christensen, *Variation in cosmic ray flux and global cloud coverage—a missing link in solar-climate relationships*, Journal of Atmospheric and Solar-Terrestrial Physics, 59 (1997) 1225.

[3] H. Svensmark, *Influence of cosmic rays on the Earth's climate*, submitted to Physical Review Letters (1997).

[4] P.V. Foukal, *The variable Sun*, Scientific American 262 (1990) 26.

[5] J.A. Eddy, *The Maunder minimum*, Science 192 (1976) 1189.

[6] E. Friis-Christensen and K. Lassen, *Length of the solar cycle: an indicator of solar activity closely associated with climate*, Science 254 (1991) 698.

[7] R.C. Willson, *Total solar irradiance trend during solar cycles 21 and 22*, Science 277 (1997) 1963.

[8] E.P. Ney, *Cosmic radiation and the weather*, Nature 183 (1959) 451.

[9] P.V. Hobbs, *Aerosol-cloud interactions*, in *Aerosol-Cloud-Climate Interactions*, International Geophysics Series, Vol. 54, ed. P.V. Hobbs, Academic Press Inc., San Diego (1993) 33.

[10] M.B. Baker, *Cloud microphysics and climate*, Science 276 (1997) 1072.

[11] D.L. Hartmann, *Radiative effects of clouds on Earth's climate*, in *Aerosol-Cloud-Climate Interactions*, International Geophysics Series, Vol. 54, ed. P.V. Hobbs, Academic Press Inc., San Diego (1993) 151.

[12] J. Beer, G.M. Raisbeck and F. Yiou, *Time variations of ^{10}Be and solar activity*, in *The Sun in Time*, eds. C.P. Sonett, M.S. Giampapa and M.S. Matthews, University of Arizona Press, Tucson (1991).

[13] J. Feynman and N.U. Crooker, *The solar wind at the turn of the century*, Nature 275 (1978) 626.

[14] M. Stuiver and P.D. Quay, *Changes in atmospheric carbon-14 attributed to a variable Sun*, Science 207 (1980) 11.

[15] D.M. Hunten, J.-C. Gérard and L.M. François, *The atmosphere's response to solar irradiation*, in *The Sun in Time*, eds. C.P. Sonett, M.S. Giampapa and M.S. Matthews, University of Arizona Press, Tucson (1991).

[16] P.E. Damon and C.P. Sonett, *Solar and terrestrial components of the atmospheric ^{14}C variation spectrum*, in *The Sun in Time*, eds. C.P. Sonett, M.S. Giampapa and M.S. Matthews, University of Arizona Press, Tucson (1991).

[17] Y.C. Lin et al., *Long term modulation of cosmic-ray intensity and solar activity cycle*, Proc. 14th International Cosmic Ray Conference, Munich, 3 (1975) 995.

[18] E. Bard et al., *Calibration of the ^{14}C timescale over the past 30,000 years using mass spectrometric U-Th ages from Barbados corals*, Nature 345 (1990) 405.

[19] A.K. Barlow and J. Latham, *A laboratory study of the scavenging of sub-micron aerosol by charged raindrops*, Quarterly Journal of the Royal Meteorological Society 109 (1983) 763.

[20] E. Segrè, *Experimental nuclear physics*, Wiley, New York (1953) 53.

[21] Nigel Calder, *Global warming—blame the Sun*, CERN seminar (December 1997).